Encapsulation of transition metal tetrahydro-Schiff base complexes in zeolite Y and their catalytic properties for the oxidation of cycloalkanes

Chun Jin [a,b], Weibin Fan [a,*], Yinjuan Jia [a], Binbin Fan [a], Jinghong Ma [a], Ruifeng Li [a,*]

[a] *Key Laboratory of Coal Science and Technology, MOE, Institute of Special Chemicals, Taiyuan University of Technology,*
79 West Yingze Street, Taiyuan 030024, PR China
[b] *Department of Chemistry, Shanxi Datong University, Datong 037009, PR China*

Abstract

A variety of transition metal (M = Cu, Co, Fe and Mn) tetrahydro-Schiff base complexes (denoted as M–[H$_4$]Schiff with Schiff = salen, salpn and salicyhexen, see Scheme 1) have been encapsulated in zeolite Y with flexible ligand method for the first time. The prepared samples were characterized with X-ray diffraction, diffuse reflectance UV–vis spectroscopy, Infrared spectroscopy, N$_2$ adsorption/desorption at −196 °C, elemental analysis, as well as thermo-gravimetry and differential-thermal analysis techniques. The formation of tetrahydro-Schiff base ligand was confirmed with ^{1}H NMR and IR spectroscopy before complexing. The prepared M–[H$_4$]Schiff/Y catalysts such as Cu–[H$_4$]salen/Y showed much higher conversion in the oxidation of cyclohexane than the corresponding M–Schiff analogues encapsulated in zeolite Y as a result of the incorporation of larger amounts and the stronger oxidation ability of tetrahydro-Schiff base complexes. In addition, the M–[H$_4$]Schiff/Y catalysts were also active for the oxidation of other cycloalkanes although their activity depended on the reaction conditions as well as the central transition metals of the complexes and the substrate molecules. It was shown that the catalytic reaction occurred via a radical mechanism. The time for the addition of H$_2$O$_2$ significantly affected the catalytic performance. Earlier (e.g. 20 min) addition of H$_2$O$_2$ than substrate molecules to the reaction system led to a drastic reduction in the catalytic activity.
© 2006 Elsevier B.V. All rights reserved.

Keywords: Transition metal tetrahydro-Schiff base complex; Zeolite Y; Encapsulation; Cyclohexane oxidation and "ship-in-a-bottle" material

1. Introduction

Catalytic oxidation of C–H bonds in saturated hydrocarbons is one of the key steps in functionalizing hydrocarbons and rapidly building functionality into a range of molecules [1,2]. This is because alcohols and ketones, like cyclohexanone, are important intermediate materials for the manufacture of many important products, such as fiber, drugs and fragrance. However, most of such oxidation reactions are still using homogeneous catalysts. From the sustainable and green chemistry point of view, heterogeneous catalysts would be attractive since they offer the advantages of easy catalyst separation, possible cat-

alyst recycle and sometimes high activity and selectivity. In this respect, encapsulation of transition metal complex in zeolites gained much interest in the last decade [1–10] since this process can give rise to the materials with both homogeneous-catalysis and heterogeneous-catalysis characters. In addition, degradation of the organic ligands, and dimerization of the transition metal complexes could occur during homogeneous catalysis reactions, resulting in a reduction in the activity, and even irreversible deactivation. In contrast, upon encapsulation in zeolites, transition metal complex molecules are encaged and site-isolated, making these complexes stable, highly active and selective for the oxidation of alkanes, alkenes, alcohols and so on. Indeed, it was found that Mn–salen/X shows high activity for the oxidation of styrene and *p*-Xylene [3,11], whereas Cu–salen is enhanced in the catalytic activity with respect to the oxidation of phenol after encapsulated in zeolite Y [12]. Corma and co-workers reported that chiral Mn(III)–salen/Y is an effective

* Corresponding authors.
E-mail addresses: fwb_2001@hotmail.com (W. Fan),
rfli@tyut.edu.cn (R. Li).
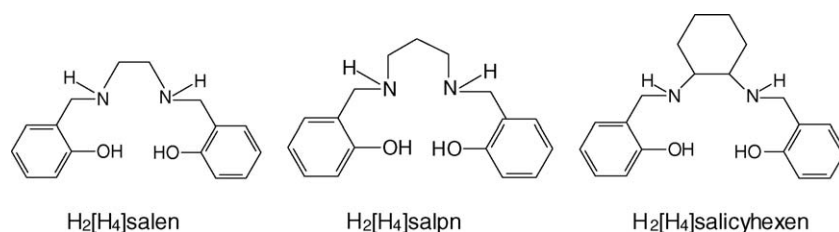
Scheme 1. The molecular structure of the tetrahydro-Schiff base ligands under study.

heterogeneous enantioselective catalyst for the epoxidation of alkenes [13].

Encapsulation of Schiff base complexes could be considered as the most extensively studied in the research field of ship-in-a-bottle materials as this type of complexes has a flexible conformation with various geometries, viz. planar, umbrella-type and stepped configurations, and as a consequence could generate different active site environments for various oxidation reactions. However, the amount of the encapsulated salen complex is very limited owing to the presence of relatively rigid C=N bond. In contrast, hydrogenation of C=N to C–N (Scheme 1), as expected, would increase N basicity and make the conformation of the complex more flexible, and hence resulting in the more ready coordination to metal centers in a folded fashion, and thus the inclusion of more Cu complex molecules, or active sites without severe blockage of the channels in zeolitic matrix. In addition, it has been shown that copper tetrahydrosalen complex (Cu–[H$_4$]salen) is also much more active than Cu–salen in the homogeneous oxidation of alkylbenzenes and cyclohexane [14]. This would make the Cu–[H$_4$]salen/Y be an effective heterogenous catalyst for the oxidation of such a type of organic substrate. Here, we report the synthesis and characterization of series of M–[H$_4$]Schiff/Y catalysts as well as their catalytic performance in the oxidation of various cycloalkanes.

2. Experimental

2.1. Preparation of samples

H$_2$Schiff (Schiff = salen, salpn and salicyhexen) ligands were prepared basically by following the procedures reported in Ref. [11,15]. Namely, 0.1 mol diamine, either ethylenediamine, propylenediamine or cyclohexenediamine, was dissolved in 25 mL ethanol. The obtained solution was then slowly added to a solution composed of 0.2 mol salicyladehyde and 150 mL ethanol under stirring conditions. The resultant solution was further refluxed for 1 h, resulting in the precipitation of a yellow solid, which was filtered and recrystallized from ethanol.

Ligands H$_2$[H$_4$]Schiff were prepared by the following method [14]: 0.01 mol H$_2$Schiff was dissolved in 60 mL methanol, followed by the addition of 0.011 mol NaBH$_4$ at ambient temperature. After 2 h of stirring, the solvent was removed by distilling under vacuum conditions. The solid product was further washed with distilled water and recrystallized from ethanol. The as-synthesized H$_2$[H$_4$]Schiff ligands were confirmed with ^{1}H NMR and FT-IR spectroscopies. The ^{1}H NMR (CDCl$_3$) of H$_2$[H$_4$]salen, H$_2$[H$_4$]salpn and H$_2$[H$_4$]salicyhexen: δ 6.7–7.2

(m, 8H), 3.9 (s, 4H), 2.8 (s, 4H); δ 6.7–7.2 (m, 8H), 3.95 (s, 4H), 2.7 (t, 4H), 1.7 (t, 2H) and δ 6.7–7.2 (m, 8H), 3.8–4.0 (s, 4H), 2.2–2.4 (t, 2H), 1.65 (d, 4H), 1.1–1.2 (m, 4H). In the infrared (IR) spectra, a band attributed to ν (N–H) was observed at 3286, 3288 and 3300 cm^{-1} for the H$_2$[H$_4$]salen, H$_2$[H$_4$]salpn and H$_2$[H$_4$]salicyhexen ligands, respectively. IR spectroscopy also shows that the spectra of the formed transition metal complexes were very similar to those of the corresponding H$_2$[H$_4$]Schiff ligands except that the bands arising from O–H stretching vibrations perturbed by the hydrogen-bonded N atom disappeared.

The procedures for the preparation of metal (M = Cu, Co, Mn and Fe) complexes are as follows: 0.01 mol H$_2$Schiff or H$_2$[H$_4$]Schiff ligands were dissolved in 50 mL ethanol, and then heated to boiling temperature. This was followed by the drop-wise addition of a solution of 0.01 mol metal salt (Cu(CH$_3$COO)$_2$·H$_2$O, Co(CH$_3$COO)$_2$·4H$_2$O, Mn(CH$_3$COO)$_2$·4H$_2$O or Fe(NO$_3$)$_3$·9H$_2$O) in 125 mL ethanol and 10 mL NaOH (2 M) aqueous solution. The resultant solution was stirred and refluxed for 1 h. After cooling, the solid product was separated by filtration and recrystallized from CHCl$_3$/petroleum ether.

M–Y was prepared by ion-exchange method. Typically, 3.2 mmol of one type of the above-mentioned metal salt was first dissolved in 400 mL deionized water. Then, 20 g Na–Y was added to the solution, and further stirred for 24 h at ambient temperature. Then, the solid fraction was filtered out, twice washed with deionized water, and dried at 120 °C for 12 h. Encapsulation of metal complex was performed with the flexible ligand method. First, M–Y was uniformly mixed with an excessive amount of H$_2$Schiff or H$_2$[H$_4$]Schiff ligands (n_{ligand}/n_{metal} = 3), and sealed into a round flask. The complexation was carried out under high vacuum conditions for 24 h at the temperatures of 150, 100, 130, 120 and 130 °C for M–salen and M–[H$_4$]salen, M–salpn, M–[H$_4$]salpn, M–salicyhexen and M–[H$_4$]salicyhexen, respectively. Uncomplexed ligands and the complex adsorbed on the exterior surface were removed by full Soxhlet extraction with acetone. The extracted sample was ion-exchanged with 0.1 M NaCl aqueous solution to remove uncoordinated Cu^{2+} ions, followed by washing with deionized water until no Cl$^-$ anions could be detected with AgNO$_3$ aqueous solution.

2.2. Characterization of samples

The structure of zeolite Y was confirmed after encapsulation of transition metal complex by a Rigaku Dmax/γA X-ray diffractometer with Cu Kα radiation (40 kV, 20 mA). IR spectra were recorded on a Perkin-Elmer Spectrum One Fourier

transform infrared spectrometer by using the conventional KBr pellet method (3 wt.%). Diffuse reflectance (DR) UV–vis spectra in the range of 200–800 nm were measured against a halon white reference standard on a Jasco V-550 UV–vis spectrophotometer equipped with an integration sphere. Thermo-gravimetry and differential-thermal analysis (TG/DTA) was performed on an ULVAC-Riko TGD 9600 thermal analysis system in flowing air (60 mL/min) at a heating rate of 10 °C/min. N_2 adsorption/desorption isotherms at −196 °C were measured on a Belsorp 18 instrument. Before measuring, the sample was pretreated at 150 °C for 6 h under high vacuum conditions. The chemical composition was determined by an inductively coupled plasma–atomic emission spectrometer (TJA Atom Scan 16). [1H] NMR spectra were recorded on a Varian INOVA-600 nuclear magnetic resonance spectrometer. The relax time was set to 1 s and 16 scans was accumulated. TMS was used as a reference.

2.3. Catalytic measurements

The liquid-phase oxidation of cycloalkanes with H_2O_2 (30% in aqueous solution) was carried out at 60 °C for 2 h under stirring conditions in a sealed autoclave (50 mL). A typical reaction mixture is as follows: 0.1 g catalyst, 18.5 mmol substrate, 19.5 mmol H_2O_2, 10 mL solvent. The product was analyzed by a GC-9A gas chromatograph equipped with a PEG packed column (3 m in length) and a flame ionization detector. Alkane conversion was determined as follows with benzyl chloride as an internal standard: Conversion (%) = 100 × {[formed cycloalkanol (mol) + formed cycloalkanone (mol)]/added cycloalkane (mol)}. Turnover number (TON) was calculated according to the formula of: TON = converted alkane (mol)/the amount of metal cations present in the added catalyst (mol).

3. Results and discussion

3.1. Preparation and characterization of samples

As already mentioned in the experimental section, encapsulation of M–Schiff base and M–[H_4]Schiff base in zeolite Y was carried out with flexible ligand method. This process has no strong influence on the structure of zeolite Y, as evidenced by XRD measurements that no obvious change in the position and the relative intensity of diffraction lines was observed after encapsulation of complexes.

Fig. 1 shows the IR spectra of Cu–Y, Cu–[H_4]salen/Y and the mechanical mixture of Cu–Y and Cu–[H_4]salen (5%) complex (denoted as (Cu–Y + Cu–[H_4]salen)). It is evident that framework vibration bands of zeolite Y dominate the spectra below 1200 cm^{-1} for all samples. The bands at 458, 564, 687 and 767 as well as 990 and 1132 cm^{-1} are attributed to T–O bending mode, double ring, symmetric stretching and asymmetric stretching vibrations, respectively. No shift was observed upon inclusion of Cu–[H_4]salen and Cu–salen complexes, further substantiating that zeolite framework remains unchanged. In addition, the band due to the bending vibration of H_2O molecules in zeolite lattices was also displayed at 1634 cm^{-1} in all the spectra. In spite of this, there is obviously a differ-
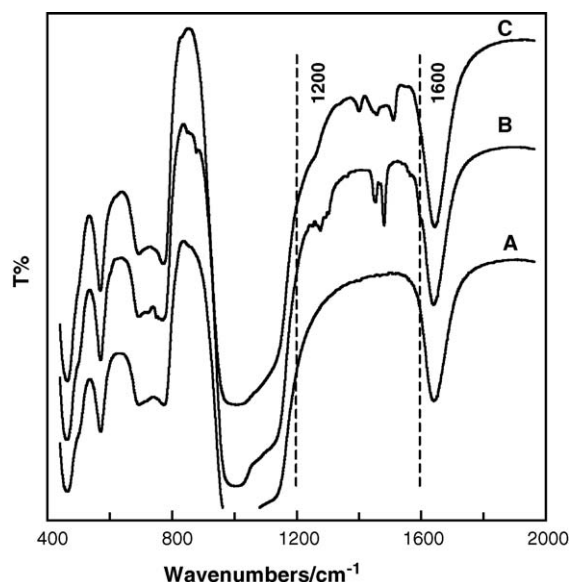

Fig. 1. FT-IR spectra of pure Cu–Y (A), the Cu–Y + Cu–[H_4]salen (5%) (B), and the Cu–[H_4]salen/Y samples (C).

ence in the range of 1200–1600 cm^{-1} among the Cu–Y sample and the Cu–[H_4]salen/Y and (Cu–Y + Cu–[H_4]salen) samples. It can be seen that all the prominent bands, assigned to C–O, C–N, and aromatic ring vibrations of ligands, were present at about 1255, 1290, 1396, 1450 and 1505 cm^{-1} in the spectra of the Cu–[H_4]salen/Y and the (Cu–Y + Cu–[H_4]salen) samples although the exact positions of these bands were not the same for these two samples probably as a result of the existence of strong interaction between zeolite framework and encapsulated complex since Cu^{2+} could form weak Cu–O bonds with zeolite lattice oxygen to give either square-pyramidal or octahedral geometry around Cu^{2+} ion [16]. In contrast, these bands were absent in the case of Cu–Y sample. In line with the Cu–[H_4]salen/Y sample, the framework IR spectra of other M–[H_4]Schiff/Y samples under study are also in agreement with their pure analogues and similar to that of the Cu–[H_4]salen/Y sample (see Fig. 1s in supplementary data), verifying that various M–[H_4]Schiff complexes have been synthesized inside zeolite Y.

DR UV–vis spectra of Cu–Y, the mechanical mixture of Na–Y + Cu–[H_4]salen (5%), Cu–salen/Y and Cu–[H_4]salen/Y were as examples shown in Fig. 2. Clearly, no band was present above 300 nm in the spectrum of Cu–Y. In contrast, three intense broad bands were observed for the Cu–[H_4]salen-containing and the Cu–salen/Y samples in the regions of 225–310, 310–420, and 430–530 nm, respectively. These bands are attributed to intra-ligand transition, ligand-to-metal charge transfer (CT) and d–d electron transitions, respectively [8,12,17]. Compared to the mechanical mixture of Na–Y + Cu–[H_4]salen (5%), the CT and particularly d–d bands considerably blue-shifted to about 350 and 440 nm, respectively, for the Cu–[H_4]salen/Y sample. This perhaps also originates from the interaction of Cu–[H_4]salen complex with zeolite framework, although this complex is located in the supercages in a neutral form. The DR UV–vis spectra of other Cu–[H_4]Schiff/Y and M–[H_4]salen/Y (with M = Co, Fe and Mn) samples are similar to that of the Cu–[H_4]salen/Y
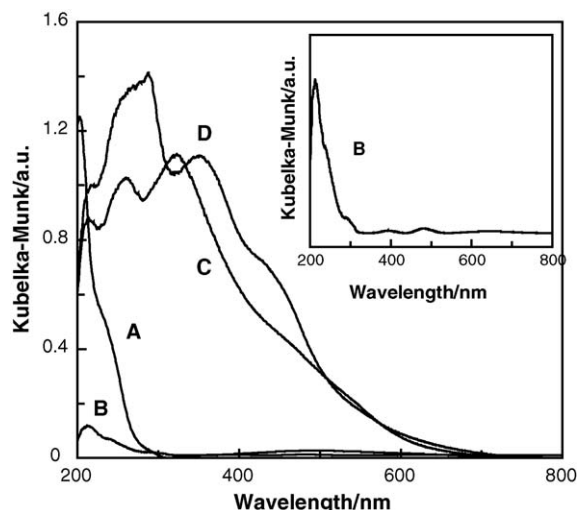
Fig. 2. DR UV–vis spectra of Cu–Y (A), Cu–[H$_4$]salen + Na–Y (5%) (B), Cu–salen/Y (C), and Cu–[H$_4$]salen/Y (D).

Fig. 3. TG (A and B) and DTA (C and D) curves of the mechanical mixture of zeolite Y and Cu–[H$_4$]salen complex (20%) (A and C) and the Cu–[H$_4$]salen/Y sample (B and D).

sample (see Fig. 2s in supplementary data), indicative of a square planer structure present in the cavity of the zeolitic matrix [17] and consistent with the IR spectroscopic result. The different positions of the CT and d–d bands for the Cu–[H$_4$]Schiff/Y samples such as Cu–[H$_4$]salen/Y from those for the Cu–Schiff/Y samples, e.g. Cu–salen/Y (318 and 470 nm), further confirms that various Cu–[H$_4$]Schiff complexes have been successfully prepared in zeolite Y.

Table 1 lists the surface area and pore volume of Cu–Y and its complex-encapsulated analogues calculated from the t-plot. As expected, encapsulation of transition metal complexes in zeolite Y led to an apparent reduction in the surface area and pore volume. Nevertheless, the decreasing degree depends on the amount of incorporated complexes as well as their molecular size and geometrical conformation inside the zeolitic host. As a result, a reduction by about 20, 50 and 75% was observed upon inclusion of Cu–salen, Cu–[H$_4$]salicyhexen, and Cu–[H$_4$]salen and Cu–[H$_4$]salph complexes, respectively.

TG/DTA analysis results are depicted in Fig. 3. Three weight-loss regions, viz. <180 °C, 260–370 °C and 370–453 °C, were present in the TG curve of the mechanical mixture of zeolite Na–Y and Cu–[H$_4$]salen (20%) complex. In contrast, two weight-loss regions of <245 °C and 300–530 °C, ascribed to desorption of physically adsorbed and occluded water, and combustion of complex molecules, respectively [9], were observed
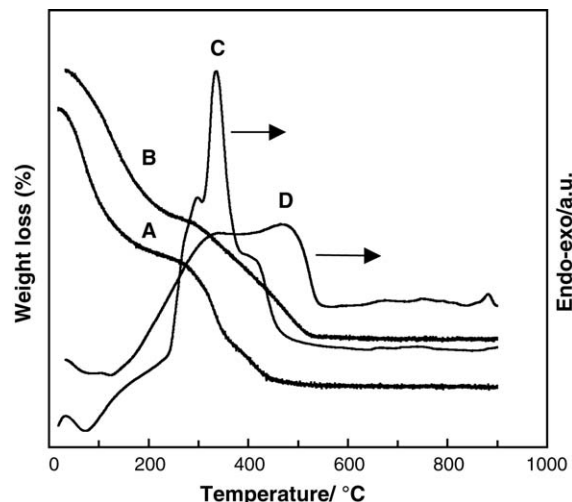
for the Cu–[H$_4$]salen/Y sample. Different from the mechanical mixture of zeolite Y and Cu–[H$_4$]salen, the continuous weight loss of Cu–[H$_4$]salen/Y in the second region has been also found for the encapsulation of other transition metal complexes in zeolites [17,18]. Regardless of this finding, the weight loss (11%) in this region is not in a good agreement with the Cu content (0.9%) in the sample, which would correspond to about 7% of the weight loss, indicating that a certain amount of uncomplexed ligands were still probably present in the samples although they suffered a full extraction with acetone. DTA curves are corresponding with TG results. In the case of Na–Y + Cu–[H$_4$]salen (20%), a very intense exothermal peak at 339 °C with two shoulder peaks (304 and 418 °C) was observed, whereas for the Cu–[H$_4$]salen/Y sample, two broad exothermal peaks around 342 and 475 °C were displayed. The much higher peak temperature of the Cu–[H$_4$]salen/Y sample than the Na–Y + Cu–[H$_4$]salen (20%) sample gives another piece of evidence for the encapsulation of Cu–[H$_4$]salen in the supercages of zeolite Y. Despite of this, the thermal stability of M–[H$_4$]Schiff complexes depends on the ligands even after they were encaged in the zeolitic matrix (not shown here).

3.2. Catalytic performance of various M–Schiff and M–[H$_4$]Schiff complexes and their encapsulated analogues in zeolite Y

Table 2 summarizes the catalytic results for the oxidation of cyclohexane over various catalysts. It shows that Cu–Y (Entry 1) was inactive for the oxidation of cyclohexane, while M–Schiff and M–[H$_4$]Schiff complexes and their encapsulated analogues in zeolite Y exhibited activity. This substantiates that the active sites are transition metal Schiff base and tetrahydro-Schiff base complexes, not metal ions. It can be seen that the catalytic oxidation ability of Cu–Schiff complexes was independent of the types of ligands (Entries 2, 6 and 10), as suggested by similar turnover numbers (TON). This also held true for the Cu–[H$_4$]Schiff complexes (Entries 4, 8 and 12). Despite of this, Cu–[H$_4$]Schiff

Table 1
Physical properties of Cu–Y and its complex-encapsulated analogues[a]

Samples	BET surface area (m^2/g)	Langmuir surface area (m^2/g)	Pore volume (mL/g)
Cu–Y	547.5	666.0	0.23
Cu–salen/Y	429.8	559.2	0.19
Cu–[H$_4$]salen/Y	129.1	180.4	0.07
Cu–[H$_4$]salph/Y	139.4	188.9	0.06
Cu–[H$_4$]salicyhexen/Y	256.9	340.5	0.11

[a] Pore volume was calculated from t-plot.

Table 2
Catalytic results for the oxidation of cyclohexane over various M–Schiff and M–[H$_4$]Schiff complexes and their encapsulated analogues in zeolite Y[a]

Entry	Catalyst	Metal content (%)	TON	Conversion (%)	Selectivity (%)	
					−ol	-one
1	Cu–Y	1.1	–	n.d.[b]	–	–
2	Cu–salen	–	113	6.1	43	57
3	Cu–salen/Y	0.6	78	4.0	26	74
4	Cu–[H$_4$]salen	–	146	7.9	49	51
5	Cu–[H$_4$]salen/Y	0.9	120	9.5	56	44
6	Cu–salpn	–	109	5.9	43	57
7	Cu–salpn/Y	0.4	76	2.3	31	69
8	Cu–[H$_4$]salpn	–	143	7.7	43	57
9	Cu–[H$_4$]salpn/Y	0.6	92	4.3	59	41
10	Cu–salicyhexen	–	109	5.9	34	66
11	Cu–salicyhexen/Y	0.6	147	7.0	47	53
12	Cu–[H$_4$]salicyhexen	–	137	7.4	41	59
13	Cu–[H$_4$]salicyhexen/Y	0.7	152	8.4	48	52
14	Co–[H$_4$]salen/Y	0.8	51	3.8	37	64
15	Fe–[H$_4$]salen/Y	0.9	7	0.6	n.d.	100
16	Mn–[H$_4$]salen/Y	0.4	–	n.d.[b]	–	–

[a] Reaction conditions: 0.1 g catalyst (0.01 mmol for pure complexes), 10 mL acetonitrile, 18.5 mmol cyclohexane, 19.5 mmol H$_2$O$_2$ (30% in aqueous solution), 60 °C, 2 h.

[b] n.d.: not detected.

complexes showed higher activity than Cu–Schiff. Upon encapsulation in zeolite Y, the catalytic oxidation ability of Cu–salen, Cu–salpn, Cu–[H$_4$]salen and Cu–[H$_4$]salpn declined, whereas that of Cu–salicyhexen and Cu–[H$_4$]salicyhexen was enhanced, as revealed by the higher TON. This is probably attributed to the strong interaction of the complex with zeolite framework after being encapsulated in the supercages of zeolite Y, consequently leading to different interaction modes of the complex with substrate molecules. Irrespective of the fact that ligands have no strong influence on the catalytic oxidation ability of the metal complexes, the catalytic activity of these complexes is highly dependent on the types of the central metals, as indicated by the considerable difference in the TON of Cu–, Co–, Fe– and Mn–[H$_4$]salen/Y (Entries 5, 14–16). Cu–[H$_4$]salen/Y gave the highest cyclohexane conversion, while Mn–[H$_4$]salen/Y had no activity. The conversion of cyclohexane over these four catalysts decreased in the order Cu–[H$_4$]salen/Y > Co–[H$_4$]salen/Y > Fe–[H$_4$]salen/Y > Mn–[H$_4$]salen/Y. This may be due to the different redox nature of the metals and the reactivity of the tetrahydrosalen complexes towards H$_2$O$_2$ [15]. Co–, Fe– and Mn–[H$_4$]salen could readily react with dioxygen to form Co–salen, Fe–salen and Mn–salen, which led to a severe reduction in activity for the oxidation of cyclohexane. In contrast, Cu–[H$_4$]salen/Y is relatively much more stable.

As expected, the amount of Cu–[H$_4$]Schiff complexes encapsulated in zeolite Y is larger than that of Cu–Schiff as a result of their more flexible framework. This is favorable for increasing cyclohexane conversion over the prepared heterogeneous catalyst. Among the tested catalysts, Cu–[H$_4$]salen/Y showed the highest cyclohexane conversion (Table 2). Therefore, herein the influence of the reaction conditions on the catalytic behavior of Cu–[H$_4$]Schiff/Y will be discussed in the following.

3.3. Influences of reaction conditions

Solvent plays an important, and sometimes decisive role in catalytic behavior because it can make different phases uniform, thus promoting mass transportation, and could also change the reaction mechanism by affecting the intermediate species, the surface properties of catalysts and reaction pathways [19,20]. It was found in our experiment that acetonitrile was the only solvent to exhibit good catalytic activity under the conditions described in the experimental section. In contrast, when methanol, ethanol, tert-butyl alcohol, acetone, methyl ethyl ketone, choloroform and water were used as solvents, no activity could be detected. Increase in reaction time to 5 h resulted in a cyclohexane conversion of 0.5% in the solvent of methyl ethyl ketone, but no activity yet in acetone.

Effect of reaction temperature on cyclohexane conversion is illustrated in Fig. 4. As expected, cyclohexane conversion increased with increasing reaction temperature although no conversion was detected when the reaction temperature was below 30 °C. However, high temperature led to a quick decomposition of H$_2$O$_2$, as a consequence, conversely lowering down the conversion. The optimum temperature was 60 °C.

Fig. 5 shows that cyclohexane conversion increased with the increase in the reaction time up to 2 h. An attempt to further increase the cyclohexane conversion by prolonging the reaction time failed: about 95% of the added H$_2$O$_2$ was consumed when the reaction was carried out for 2 h.

Another factor affecting the cyclohexane conversion was found to be the amount of the catalyst. When 0.025 g catalyst was added to the reaction system, no activity could be detected under the typical reaction conditions as described above. However, an increase in the catalyst amount to 0.075 g led to the cyclohexane conversion reaching 9.4%, which is similar to the value achieved with 0.1 g catalyst employed (Table 2).
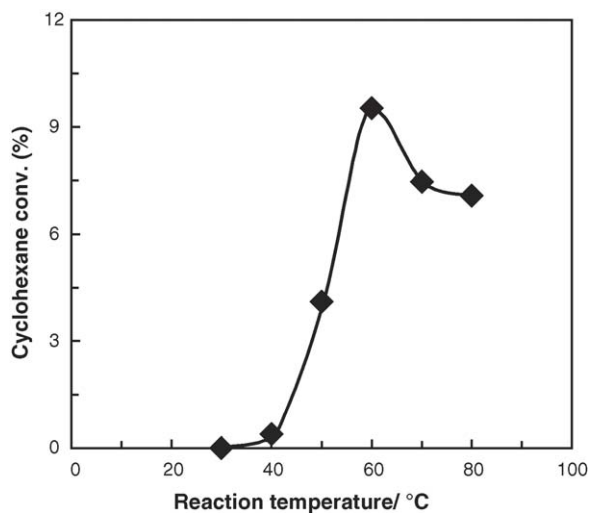
Fig. 4. Cyclohexane conversion vs. the reaction temperature for the oxidation of cyclohexane over Cu–[H$_4$]salen/Y (reaction conditions: 0.1 g catalyst, 10 mL acetonitrile, 18.5 mmol cyclohexane, 19.5 mmol H$_2$O$_2$ (30% in aqueous solution), 2 h).

The catalytic stability of Cu–[H$_4$]Schiff/Y was further investigated with Cu–[H$_4$]salen/Y as an example. Fig. 6 depicts the catalytic results of Cu–[H$_4$]salen/Y for the oxidation of cyclohexane within four repeated runs with the catalyst/substrate/H$_2$O$_2$/acetonitrile ratio maintained at the same level. It is clear that cyclohexane conversion progressively lowered down. This is due to the degradation and/or the oxidative dehydrogenation of the Cu–[H$_4$]salen complex to Cu–salen under the current reaction conditions. This was supported by the result that no apparent increase in the cyclohexane conversion was observed after separating the catalyst from the reaction liquid by centrifugation when the reaction was carried out for 1 h. The cyclohexane conversion was 6.0% at the reaction time of 1 h, which is comparable to that (6.5%) obtained by the reaction
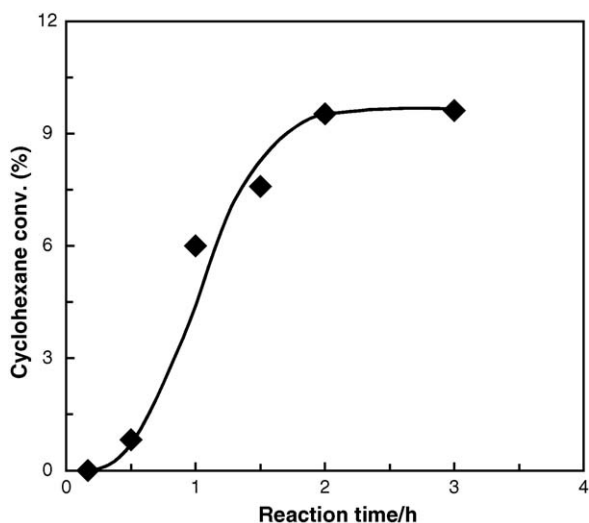

Fig. 5. Cyclohexane conversion vs. the reaction time for the oxidation of cyclohexane over Cu–[H$_4$]salen/Y (reaction conditions: 0.1 g catalyst, 10 mL acetonitrile, 18.5 mmol cyclohexane, 19.5 mmol H$_2$O$_2$ (30% in aqueous solution), 60 °C).
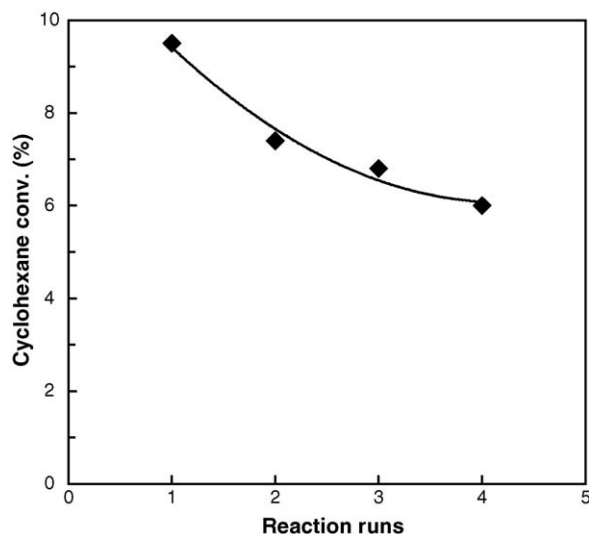

Fig. 6. Cyclohexane conversion obtained over Cu–[H$_4$]salen/Y within four repeated reaction runs (reaction conditions: 60 °C, 2 h, the catalyst/substrate/H$_2$O$_2$/solvent ratio was maintained at the same level of 0.1 g/18.5 mmol/19.5 mmol/10 mL).

for further 1 h after removing the catalyst. Nevertheless, the catalytic activity of the Cu–[H$_4$]salen/Y catalyst would be stable after four repeated runs, and maintained about 6% in cyclohexane oxidation, being 1.5 times of that obtained with the fresh Cu–salen/Y catalyst, as indicated by the function of cyclohexane conversion versus reaction runs. This proves that encapsulation of Cu–[H$_4$]salen in zeolite Y led to the formation of a reusable, and therefore, an environmentally benign heterogeneous catalyst although the oxidation ability of this complex was not enhanced.

3.4. Catalytic properties of Cu–[H$_4$]salen/Y for oxidation of various cycloalkanes

Cu–[H$_4$]salen/Y was active not only for the oxidation of cyclohexane but also for the oxidation of other cycloalkanes (Table 3). The higher conversion of cyclohexane than that of cyclopentane is anticipated since the reaction of cycloalkane oxidation is electrophilic. However, with respect to oxidation of the cycloalkanes bulkier than cyclohexane, the conversion decreased with increasing molecular size of substrates. This is contrary to the electronic effect since the molecular rings of the studied substrates here are all nearly in one plane without significant distortion. This could be attributed to the occurrence of the

Table 3
Catalytic results for the oxidation of various cycloalkanes over Cu–[H$_4$]salen/Y[a]

Entry	Substrate	Conversion (%)	Selectivity (%)	
			-ol	-one
1	Cyclopentane	6.5	31	69
2	Cyclohexane	9.5	56	44
3	Cycloheptane	8.3	16	84
4	Methylcyclohexane	5.7	46	54
5	Cyclooctane	7.6	12	88

[a] Reaction conditions: 0.1 g catalyst, 10 mL acetonitrile, 18.5 mmol substrate, 19.5 mmol H$_2$O$_2$ (30% in aqueous solution), 60 °C, 2 h.

reaction inside zeolite micropores. Although the pore opening (7.4 Å) of zeolite Y is large enough to allow all of the studied substrate molecules to diffuse into the channels, the access of these molecules to the active site of Cu–[H$_4$]salen complex encapsulated in the supercages becomes more difficult with the molecular size because the complex is too large to leave more space for accommodation of the bulkier substrates. Accordingly, the larger the substrate molecule, the lower the substrate conversion. This suggests that no leaching of Cu–[H$_4$]salen complex from the interior of the zeolite host to the solution occurred and that the complex molecules attached on external surface play a minute role in the overall catalytic process. As we know, all the enzymatic systems have a common feature of the active sites being confined in a space defined by the tertiary protein structure. Our work bio-mimics this strategy; that is, the rigid inorganic zeolite framework defines the reaction cavity surrounding the active sites of transition metal complexes.

It was found that in the presence of hydroquinone (2 mmol), an effective radical scavenger, cyclohexane conversion drastically decreased from 9.5 to 1.5% under the same reaction conditions (Fig. 7). This is consistent with the oxidation of cyclohexane occurred by a radical mechanism. Table 3 shows that the -one to -ol molar ratio of the products obtained from the oxidation of cyclohexane and methylcyclohexane was in the range from 0.8 to 1.5 for most of the studied M–[H$_4$]Schiff/Y catalysts, suggesting that the Russell termination mechanism might predominate the oxidation process [21,22]. Nevertheless, Cu–salen/Y and Cu–salicyhexen/Y gave higher one/ol ratios (>2.2) (Table 2). In addition, it was also found that the one/ol molar ratio in the products also depended on the substrate molecules when Cu–[H$_4$]salen/Y served as a catalyst. The one/ol ratio of the product formed from cyclopentane oxidation was about 2.2. In contrast, cycloheptane and cyclooctane as substrates resulted in
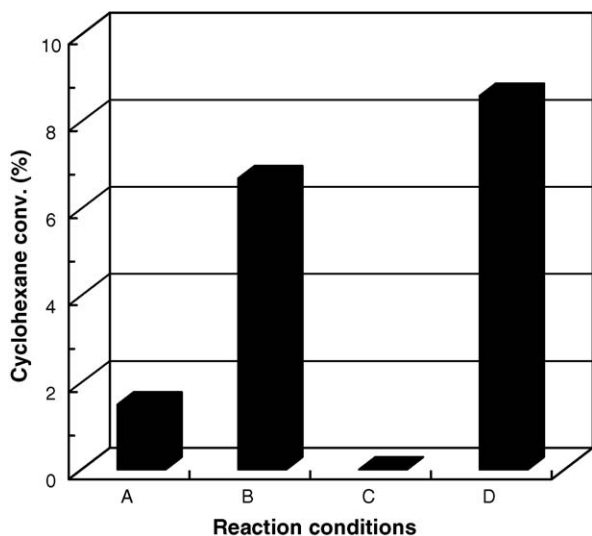
the formation of products with an one/ol ratio of 5.0 and 7.6, respectively (Table 3). This seems to support that the oxidation occurred via a heterolytic pathway [21,23]. The detailed reaction mechanism for the oxidation of different cycloalkanes is not clear yet for the moment. This needs further kinetic study and in situ-following the reaction process by various spectroscopy techniques such as DR UV–vis and ESR. This work is in progress.

Unexpectedly, cyclohexane conversion decreased to 6.7% when H$_2$O$_2$ had first reacted for 10 min prior to addition of the substrate (Fig. 7). In particular, no activity could be detected when cyclohexane was added after 20 min. However, when H$_2$O$_2$ was added 20 min after the introduction of the substrate molecule, the conversion reached 8.6%. This might be accounted for by the following assumption: the decomposition of H$_2$O$_2$ probably occurred very quickly and/or the formed free radicals and molecular oxygen were unstable, consequently resulting in the decrease in activity, and even deactivation when H$_2$O$_2$ was added to the reaction system before cyclohexane. In contrast, this problem would be avoided to a large extent if cyclohexane was first added since once free radicals and molecular oxygen formed from H$_2$O$_2$, they could auto-oxidize the substrate molecules. The slight decrease in the activity may be due to adsorption of some cyclohexane molecules on the active sites, somewhat hindering the formation of free radicals and molecular oxygen. Therefore, the substrate molecules and H$_2$O$_2$ should be simultaneously added into the reaction system.

4. Conclusions

Series of M–Schiff and M–[H$_4$]Schiff complexes have been successfully encapsulated in the supercages of zeolite Y, as evidenced by IR, DR UV–vis, ^{1}H NMR, N$_2$ adsorption/desorption at −196 °C, and TG/DTA characterization results. M–[H$_4$]Schiff/Y catalysts show much higher activity in the oxidation of cycloalkanes than the corresponding M–Schiff/Y catalysts as a result of the incorporation of more complexes molecules and their intriguing oxidation ability. Nevertheless, the catalytic performance of the M–[H$_4$]Schiff/Y catalysts is closely related to the type of transition metals because of the different redox nature of transition metals and the different oxidative dehydrogenation activity of the formed complexes towards oxygen. Cu–[H$_4$]Schiff/Y catalysts, such as Cu–[H$_4$]salen/Y, are highly active for the oxidation of cycloalkanes, and also relatively stable. The reaction conditions have a drastic influence on the catalytic activity, and acetonitrile is the solvent of choice. It was shown that a radical mechanism predominates the catalytic process. The addition time of H$_2$O$_2$ strongly affects the catalytic performance. Simultaneous addition of substrate molecules and H$_2$O$_2$ is necessary for acquiring high activity.

Fig. 7. Catalytic results for the oxidation of cyclohexane over Cu–[H$_4$]salen/Y under different conditions: (A) in the presence of 2 mmol hydroquinone; (B) cyclohexane was added after addition of H$_2$O$_2$ for 10 min; (C) cyclohexane was added after addition of H$_2$O$_2$ for 20 min; (D) cyclohexane was added before addition of H$_2$O$_2$ for 20 min (reaction conditions: 0.1 g catalyst, 10 mL acetonitrile, 18.5 mmol cyclohexane, 19.5 mmol H$_2$O$_2$ (30% in aqueous solution), 60 °C, 2 h).

Appendix A. Supplementary data

Supplementary data associated with this article can be found, in the online version, at doi:10.1016/j.molcata.2005.12.035.

References

[1] F. Farzaneh, M. Majidian, M. Ghandi, J. Mol. Catal. A 148 (1999) 227.
[2] E.L. Pires, J.C. Magalhaes, U. Schuchardt, Appl. Catal. A 203 (2000) 231.
[3] C.R. Jacob, S.P. Varkey, P. Ratnasamy, Microporous Mesoporous Mater. 22 (1998) 465.
[4] B. Zhan, X. Li, Chem. Commun. (1998) 349.
[5] K.J. Balkus Jr., M. Eissa, R. Levado, J. Am. Chem. Soc. 117 (1995) 10753.
[6] T. Kimura, A. Fukuoka, M. Ichikawa, Catal. Lett. 4 (1990) 279.
[7] B. Fan, W. Fan, R. Li, Stud. Surf. Sci. Catal. 135 (2001) 297.
[8] B. Fan, W. Cheng, R. Li, Stud. Surf. Sci. Catal. 135 (2001) 250.
[9] B. Fan, W. Fan, R. Li, J. Mol. Catal. A 201 (2003) 137.
[10] T. Joseph, S.B. Halligudi, C. Satyanarayan, D.P. Sawant, S. Gopinathan, J. Mol. Catal. A 168 (2001) 87.
[11] C.R. Jacob, S.P. Varkey, P. Ratnasamy, Appl. Catal. A 182 (1999) 91.
[12] C.R. Jacob, S.P. Varkey, P. Ratnasamy, Appl. Catal. A 168 (1998) 353.
[13] M.J. Sabater, A. Corma, A. Domenech, V. Fornes, H. Garcia, Chem. Commun. (1997) 1285.
[14] S. Velusamy, T. Punniyamurthy, Tetrahedron Lett. 44 (2003) 8955.
[15] A. Bottcher, H. Elias, E. Jager, H. Langfelderova, M. Mazur, L. Muller, H. Paulus, P. Pelikan, M. Rudoph, M. Valko, Inorg. Chem. 32 (1993) 4131.
[16] S. Koner, Chem. Commun. (1998) 593.
[17] M.R. Maurya, S.J.J. Titinchi, S. Chand, Appl. Catal. A: Gen. 228 (2002) 177.
[18] S.P. Varkey, C. Ratnasamy, P. Ratnasamy, J. Mol. Catal. A 135 (1998) 295.
[19] A. Corma, P. Esteve, A. Martinez, J. Catal. 162 (1996) 11.
[20] W. Fan, P. Wu, T. Tatsumi, J. Phys. Chem. B, submitted for publication.
[21] A.A. Valente, P. Brandao, Z. Lin, F. Goncalves, I. Portugal, M.W. Anderson, J. Rocha, Stud. Surf. Sci. Catal. 135 (2001) 368.
[22] G.A. Russell, J. Am. Chem. Soc. 79 (1957) 3871.
[23] J.D. Chen, J. Dakka, R.A. Sheldon, Appl. Catal. A 108 (1994) L1.